

**SYNTHESIS AND CHARACTERIZATION OF OXIDE CONDUCTORS IN
PbO-Bi₂O₃-M₂O₅ (M = V, P, As)**

LEE CHIU SZE

**DOCTOR OF PHILOSOPHY
UNIVERSITI PUTRA MALAYSIA**

2004

**SYNTHESIS AND CHARACTERIZATION OF OXIDE CONDUCTORS IN
PbO-Bi₂O₃-M₂O₅ (M = V, P, As)**

By

LEE CHIU SZE

**Thesis Submitted to the School of Graduate Studies, Universiti Putra Malaysia,
in Fulfilment of the Requirements for the Degree of Doctor of Philosophy**

April 2004

Abstract of thesis presented to the Senate of Universiti Putra Malaysia in fulfilment of the requirements for the degree of Doctor of Philosophy

**SYNTHESIS AND CHARACTERIZATION OF OXIDE CONDUCTORS IN
PbO-Bi₂O₃-M₂O₅ (M = V, P, As)**

By

LEE CHIU SZE

April 2004

Chairperson: Professor Lee Chnoong Kheng, Ph.D.

Faculty: Science and Environmental Studies

Materials of compositions PbBi₆M₂O₁₅ and (PbO)_n(BiMO₄), where M = V, P, As and n = 1, 2, 4 were prepared via solid state reaction. These materials were characterised using X-ray diffraction (XRD), density measurement, inductively coupled plasma-atomic emission spectrometry (ICP-AES), ac impedance spectroscopy, differential thermal analysis (DTA), thermogravimetry analysis (TGA), Fourier-transform infrared spectroscopy (FT-IR) and scanning electron microscopy (SEM).

Complete solid solution series were obtained in the PbBi₆V₂O₁₅-PbBi₆P₂O₁₅, PbBi₆V₂O₁₅-PbBi₆As₂O₁₅ and PbBi₆P₂O₁₅-PbBi₆As₂O₁₅ systems. All the materials were isostructural, and crystallised in orthorhombic symmetry. However, the cell parameter a of these materials was twice those reported in JCPDS. The conductivity of these materials decreased in the order of PbBi₆V₂O₁₅ > PbBi₆As₂O₁₅ > PbBi₆P₂O₁₅. PbBi₆V₂O₁₅ is an oxide ion conductor as it has a transference number of 0.8 above 650°C.

Substitution of Sr for Pb in $\text{PbBi}_6\text{V}_2\text{O}_{15}$ resulted in the formation a new material of $\text{SrBi}_6\text{V}_2\text{O}_{15}$ with higher conductivity. On the other hand, Pb in both $\text{PbBi}_6\text{V}_2\text{O}_{15}$ and $\text{PbBi}_6\text{As}_2\text{O}_{15}$ could be replaced by Na and Bi, resulting in the formation of $\text{NaBi}_{13}\text{V}_4\text{O}_{30}$ and $\text{NaBi}_{13}\text{As}_4\text{O}_{30}$. Besides successfully suppressing the phase transition observed in $\text{PbBi}_6\text{V}_2\text{O}_{15}$, these materials had higher conductivity compared to that of $\text{PbBi}_6(\text{V}/\text{As})_2\text{O}_{15}$. The conductivity of these materials was in the range of $\sim 10^{-3} \text{ ohm}^{-1} \text{ cm}^{-1}$ at 800°C . Conductivity decreased in the order of $\text{NaBi}_{13}\text{V}_4\text{O}_{30} > \text{SrBi}_6\text{V}_2\text{O}_{15} > \text{PbBi}_6\text{V}_2\text{O}_{15}$. These materials appeared to be oxide ion conductors.

Complete solid solution series were formed in the Pb_2BiPO_6 - $\text{Pb}_2\text{BiAsO}_6$, Pb_4BiPO_8 - Pb_4BiVO_8 , Pb_4BiPO_8 - $\text{Pb}_4\text{BiAsO}_8$ and Pb_4BiVO_8 - $\text{Pb}_4\text{BiAsO}_8$ systems. The properties determined generally agreed with those reported; these materials were mixed oxide ion conductors. The conductivity decreased in the order of $\text{Pb}_2\text{BiMO}_6 > \text{PbBiMO}_5 > \text{Pb}_4\text{BiMO}_8$, and $\text{V} > \text{As} > \text{P}$.

Abstrak tesis yang dikemukakan kepada Senat Universiti Putra Malaysia sebagai memenuhi keperluan untuk ijazah kedoktoran

**SINTESIS DAN PENCIRIAN KONDUKTOR OKSIDA DALAM
PbO-Bi₂O₃-M₂O₅ (M = V, P, As)**

Oleh

LEE CHIU SZE

April 2004

Pengerusi: Profesor Lee Chnoong Kheng, Ph.D.

Fakulti: Sains and Pengajian Alam Sekitar

Bahan-bahan dengan komposisi PbBi₆M₂O₁₅ dan (PbO)_n(BiMO₄), di mana M = V, P, As dan n = 1, 2, 4 telah disediakan melalui tindak balas keadaan pepejal. Bahan-bahan telah dicirikan dengan menggunakan pembelauan sinar-X (XRD), pengukuran ketumpatan, plasma aruhan ke-duaan-spektroskopi penyebaran atom (ICP-AES), spektroskopi impedans ac, analisis perbezaan terma (DTA), analisis termogravimetri (TGA), spektroskopi inframerah transformasi Fourier (FT-IR) dan spektroskopi imbasan electron (SEM).

Larutan pepejal lengkap telah diperolehi dalam sistem PbBi₆V₂O₁₅-PbBi₆P₂O₁₅, PbBi₆V₂O₁₅-PbBi₆As₂O₁₅ dan PbBi₆P₂O₁₅-PbBi₆As₂O₁₅. Semua bahan mempunyai simetri yang sama, dan mereka dihablurkan dalam simetri ortorombik. Tetapi, parameter unit cell a bahan-bahan ini adalah dua kali ganda daripada yang dilaporkan dalam JCPDS. Kekonduksian bahan-bahan ini menurun dalam susunan PbBi₆V₂O₁₅ > PbBi₆As₂O₁₅ > PbBi₆P₂O₁₅. PbBi₆V₂O₁₅ adalah konduktor ion oksida disebabkan ia mempunyai nombor pindahan 0.8 pada suhu 650°C ke atas.

Pertukaran Sr untuk Pb dalam $\text{PbBi}_6\text{V}_2\text{O}_{15}$ telah menghasilkan pembentukan satu bahan baru $\text{SrBi}_6\text{V}_2\text{O}_{15}$ dengan kekonduksian yang lebih tinggi. Selain itu, Pb dalam $\text{PbBi}_6\text{V}_2\text{O}_{15}$ and $\text{PbBi}_6\text{As}_2\text{O}_{15}$ boleh diganti dengan Na dan Bi, mengakibatkan panghasilan $\text{NaBi}_{13}\text{V}_4\text{O}_{30}$ dan $\text{NaBi}_{13}\text{As}_4\text{O}_{30}$. Selain daripada berjaya menghilangkan peralihan fasa yang dilihat dalam $\text{PbBi}_6\text{V}_2\text{O}_{15}$, bahan-bahan ini mempunyai kekonduksian yang lebih tinggi daripada $\text{PbBi}_6(\text{V}/\text{As})_2\text{O}_{15}$. Kekonduksian bahan-bahan ini adalah dalam lingkungan $\sim 10^{-3} \text{ ohm}^{-1} \text{ cm}^{-1}$ pada suhu 800°C . Kekonduksian menurun dalam susunan $\text{NaBi}_{13}\text{V}_4\text{O}_{30} > \text{SrBi}_6\text{V}_2\text{O}_{15} > \text{PbBi}_6\text{V}_2\text{O}_{15}$. Bahan-bahan ini merupakan konduktor ion oksida.

Larutan pepejal lengkap telah dibentuk dalam sistem $\text{Pb}_2\text{BiPO}_6\text{-Pb}_2\text{BiAsO}_6$, $\text{Pb}_4\text{BiPO}_8\text{-Pb}_4\text{BiVO}_8$, $\text{Pb}_4\text{BiPO}_8\text{-Pb}_4\text{BiAsO}_8$ dan $\text{Pb}_4\text{BiVO}_8\text{-Pb}_4\text{BiAsO}_8$. Kelakuan yang ditentukan adalah agak sama dengan yang dilaporkan; bahan-bahan ini merupakan konduktor campuran ion oksida. Kekonduksian menurun dalam susunan $\text{Pb}_2\text{BiMO}_6 > \text{PbBiMO}_5 > \text{Pb}_4\text{BiMO}_8$, dan $\text{V} > \text{As} > \text{P}$.

ACKNOWLEDGEMENTS

First of all I would like to express my deep gratitude to my supervisor, Professor Dr. Lee Chnoong Kheng, for her constant encouragement, constructive suggestions and continuous discussion throughout the project. I would also like to extend my sincere appreciation to my co-supervisors Assoc. Prof. Dr. Zulkarnain Zainal and Assoc. Prof. Dr. Mansor Hashim for their guidance, suggestions and comments throughout the research work.

My special thanks are due to Professor Dr. A. R. West for helpful discussions and comments on this work. Besides, I would also like to thank Dr. Akiteru Watanabe for his assistance in carrying out the transference number measurements.

Particular thanks are also extended to Madam Choo (ICP-AES), Mr. Kamal Margona (DTA, TGA), Mdm. Rusnani Amirudin (IR), Mr. Ho Oi Kuan, Mrs. Azilah Ab. Jalil, Mr. Rafiez (SEM) and all the laboratory technicians for their help and guidance in operating the instruments.

I am extremely grateful to all my friends, Miss Lim Ei Bee, Miss Sim Leng Tze, Miss Lee Siew Ling, lab mates and all my friends in UPM for their constant encouragements and help throughout these few years.

The financial support from the Ministry of Science and Technology and Universiti Putra Malaysia is gratefully acknowledged. Without this support, it is impossible for

me to pursue this project with success. Lastly, I would also like to extend my gratitude to the Malaysian government for granting me the PASCA scholarship.

Last but not least, I would like to give my sincere thanks to all the members of my family and Dr. Lim Kean Pah for their love, continuous support, encouragement and understanding.

LIST OF ABBREVIATIONS / NOTATIONS / GLOSSARY OF TERMS

3D	three dimensions
ac	alternating current
BIMEVOX	bismuth metal vanadium oxide
dc	direct current
DTA	differential thermal analysis
FT-IR	Fourier-transform infrared spectroscopy
ICDD	international centre for diffraction data
ICP-AES	inductively coupled plasma-atomic emission spectrometry
JCPDS	Joint Committee on Powder Diffraction Standards
μ PDSM	micro powder diffraction search / match
SEM	scanning electron microscopy
SOFC	solid oxide fuel cell
TGA	thermogravimetry analysis
XRD	X-ray diffraction
YSZ	yttria stabilised zirconia
a, b, c, α , β , γ	lattice constant
A	area
A_w	Warburg coefficient
C	capacitance
C_b	bulk capacitance
C_{dl}	double-layer capacitance
C_{gb}	grain boundary capacitance
C_o	vacuum capacitance

d	d-spacing
D	density
e	charge of the conducting species
ϵ_0	permittivity of free space
E	electric field
E_a	activation energy
ϵ'	relative permittivity
ϵ^*	complex permittivity
f	frequency
F	Faraday constant
h, k, l	Miller indice
I	current
j	flux of charge
J	density of the current
l	thickness
λ	wavelength
M	dopant introduced
M'	real part of modulus
M''	imaginary part of modulus
M^*	complex modulus
μ	mobility of the species
P'	partial pressure to be measured
P''	reference partial pressure
R	resistance

R	universal gas constant
R_b	bulk resistance
R_{gb}	grain boundary resistance
σ	conductivity
t	transference number
T	temperature
θ	Bragg angle
τ	electrical relaxation times
ω	angular frequency
Z	formula unit
Z	impedance
Z'	real part of impedance
Z''	imaginary part of impedance
Z^*	complex impedance

TABLE OF CONTENTS

	Page
ABSTRACT	ii
ABSTRAK	iv
ACKNOWLEDGEMENTS	vi
APPROVAL	viii
DECLARATION	x
LIST OF TABLES	xiv
LIST OF FIGURES	xvii
LIST OF ABBREVIATIONS / NOTATIONS / GLOSSARY OF TERMS	xxx

CHAPTER

1	INTRODUCTION	1.1
	1.1 Ionic Conductivity and Solid Electrolytes	1.3
	1.1.1 Ionic Conduction	1.6
	1.2 Solid Solutions	1.7
	1.3 Oxide Ion Conductors and Their Applications	1.8
	1.3.1 Oxygen Sensors	1.10
	1.3.2 Solid Oxide Fuel Cell (SOFC)	1.14
	1.4 Objectives	
2	LITERATURE REVIEW	
	2.1 Oxide Ion Conductors	2.1
	2.2 Pure Bismuth Oxide	2.2
	2.3 Bi ₂ O ₃ -based Binary Systems	2.7
	2.4 Bi ₂ O ₃ -based Ternary Systems	2.14
3	MATERIALS AND METHODS	
	3.1 Sample Preparation	3.1
	3.1.1 PbBi ₆ (V/P/As) ₂ O ₁₅ , Pb _{1-x} Sr _x Bi ₆ (V/As) ₂ O ₁₅ and NaBi ₁₃ (V/P/As) ₄ O ₃₀ Solid Solutions	3.1
	3.1.2 PbBi(V/As)O ₅ , Pb _{1-x} Sr _x BiVO ₅ , Pb ₂ Bi(V/P/As)O ₆ and Pb ₄ Bi(V/P/As)O ₈ Solid Solutions	3.3
	3.2 Analysis and Characterisation	3.6
	3.2.1 X-ray Diffraction (XRD)	3.6
	3.2.2 Density Measurement	3.10
	3.2.3 Elemental Analysis – Inductively Coupled Plasma-Atomic Emission Spectrometry (ICP-AES)	3.11
	3.2.4 Electrical Properties	3.14
	3.2.5 Thermal Analysis	3.27
	3.2.6 Fourier-transform Infrared Spectroscopy (FT-IR)	3.29

3.2.7	Scanning Electron Microscopy (SEM)	3.30
3.3	Phase Stability	3.31
3.3.1	Melting Point	3.31
3.3.2	Slow Cool	3.31
4	RESULTS AND DISCUSSION	
4.1	$\text{PbBi}_6(\text{V/P/As})_2\text{O}_{15}$ Solid Solutions	4.1
4.1.1	Phase Purity	4.1
4.1.2	Density	4.11
4.1.3	Melting Point and Phase Stability	4.11
4.1.4	Elemental Analysis – ICP-AES	4.15
4.1.5	Fourier-transform Infrared Spectroscopy	4.19
4.1.6	Thermal Analysis	4.23
4.1.7	Scanning Electron Microscopy	4.29
4.1.8	Electrical Properties	4.32
4.2	$\text{Pb}_{1-x}\text{Sr}_x\text{Bi}_6(\text{V/As})_2\text{O}_{15}$ Solid Solutions	4.54
4.2.1	Phase Purity	4.54
4.2.2	Density	4.60
4.2.3	Melting Point and Phase Stability	4.63
4.2.4	Elemental Analysis – ICP-AES	4.63
4.2.5	Fourier-transform Infrared Spectroscopy	4.65
4.2.6	Thermal Analysis	4.65
4.2.7	Scanning Electron Microscopy	4.67
4.2.8	Electrical Properties	4.69
4.3	$\text{NaBi}_{13}(\text{V/P/As})_4\text{O}_{30}$ Solid Solutions	4.82
4.3.1	Phase Purity	4.82
4.3.2	Density	4.88
4.3.3	Melting Point and Phase Stability	4.88
4.3.4	Elemental Analysis – ICP-AES	4.93
4.3.5	Fourier-transform Infrared Spectroscopy)	4.94
4.3.6	Thermal Analysis	4.96
4.3.7	Scanning Electron Microscopy	4.96
4.3.8	Electrical Properties	4.100
4.4	$(\text{PbO})_n[\text{Bi}(\text{V/As})\text{O}_4]$, $n = 1$, and Their Solid Solutions	4.118
4.4.1	Phase Purity and Crystal Structure	4.118
4.4.2	Melting Point and Phase Stability	4.123
4.4.3	Elemental Analysis – ICP-AES	4.126
4.4.4	Fourier-transform Infrared Spectroscopy	4.126
4.4.5	Thermal Analysis	4.128
4.4.6	Scanning Electron Microscopy	4.128
4.4.7	Electrical Properties	4.128
4.5	$(\text{PbO})_n[\text{Bi}(\text{V/P/As})\text{O}_4]$, $n = 2$, and Their Solid Solutions	4.142
4.5.1	Phase Purity and Crystal Structure	4.142
4.5.2	Density	4.150
4.5.3	Melting Point and Phase Stability	4.155
4.5.4	Elemental Analysis – ICP-AES	4.156
4.5.5	Fourier-transform Infrared Spectroscopy	4.156
4.5.6	Thermal Analysis	4.161

4.5.7	Scanning Electron Microscopy	4.165
4.5.8	Electrical Properties	4.168
4.6	$(\text{PbO})_n[\text{Bi}(\text{V/P/As})\text{O}_4]$, $n = 4$, and Their Solid Solutions	4.183
4.6.1	Phase Purity and Crystal Structure	4.183
4.6.2	Density	4.191
4.6.3	Melting Point and Phase Stability	4.191
4.6.4	Elemental Analysis – ICP-AES	4.198
4.6.5	Fourier-transform Infrared Spectroscopy	4.198
4.6.6	Thermal Analysis	4.203
4.6.7	Scanning Electron Microscopy	4.203
4.6.8	Electrical Properties	4.205
4.7	Summary	4.219
5	CONCLUSIONS	5.1
	REFERENCES	R.1
	APPENDICES	A.1
	BIODATA OF THE AUTHOR	B.1

LIST OF TABLES

Table		Page
3.1	List of samples prepared in $\text{PbBi}_6(\text{V}/\text{As})_2\text{O}_{15}$, $\text{Pb}_{1-x}\text{Sr}_x\text{Bi}_6(\text{V}/\text{As})_2\text{O}_{15}$ and $\text{NaBi}_{13}(\text{V}/\text{P}/\text{As})_4\text{O}_{30}$ solid solution series	3.2
3.2	List of samples prepared in $\text{PbBi}(\text{V}/\text{As})\text{O}_5$, $\text{Pb}_{1-x}\text{Sr}_x\text{BiVO}_5$, $\text{Pb}_2\text{Bi}(\text{V}/\text{P}/\text{As})\text{O}_6$ and $\text{Pb}_4\text{Bi}(\text{V}/\text{P}/\text{As})\text{O}_8$ solid solution series	3.5
3.3	Wavelength used and detection limit for each element in the elemental analysis by ICP-AES	3.13
3.4	Capacitance values and their possible interpretation (Irvine et al., 1990)	3.21
4.1	Melting points of x in $\text{PbBi}_6\text{V}_{2-x}\text{P}_x\text{O}_{15}$, $\text{PbBi}_6\text{V}_{2-x}\text{As}_x\text{O}_{15}$ and $\text{PbBi}_6\text{P}_{2-x}\text{As}_x\text{O}_{15}$ solid solutions	4.15
4.2	Atomic % of the elements calculated from ICP-AES analysis of $\text{PbBi}_6\text{V}_2\text{O}_{15}$, $\text{PbBi}_6\text{P}_2\text{O}_{15}$ and $\text{PbBi}_6\text{As}_2\text{O}_{15}$	4.16
4.3	Atomic % of the elements determined from ICP-AES analysis of selected samples in $\text{PbBi}_6\text{V}_{2-x}\text{P}_x\text{O}_{15}$ solid solutions	4.17
4.4	Atomic % of the elements determined from ICP-AES analysis of selected samples in $\text{PbBi}_6\text{V}_{2-x}\text{As}_x\text{O}_{15}$ solid solutions	4.18
4.5	Atomic % of the elements determined from ICP-AES analysis of selected samples in $\text{PbBi}_6\text{P}_{2-x}\text{As}_x\text{O}_{15}$ solid solutions	4.19
4.6	Vibrational frequencies for M-O stretching (Nakamoto, 1970)	4.23
4.7	Phase transition temperatures of x in $\text{PbBi}_6\text{V}_{2-x}\text{P}_x\text{O}_{15}$	4.28
4.8	Phase transition temperatures of x in $\text{PbBi}_6\text{V}_{2-x}\text{As}_x\text{O}_{15}$	4.29
4.9	Phase transition temperatures of x in $\text{PbBi}_6\text{P}_{2-x}\text{As}_x\text{O}_{15}$	4.29
4.10	Grain size of x in $\text{PbBi}_6\text{V}_{2-x}\text{P}_x\text{O}_{15}$	4.31
4.11	Grain size of x in $\text{PbBi}_6\text{V}_{2-x}\text{As}_x\text{O}_{15}$	4.32
4.12	Conductivity values at 550 and 800°C and the activation energy for $\text{PbBi}_6\text{P}_2\text{O}_{15}$ at different atmospheres	4.46
4.13	Conductivity values at 550 and 800°C and the activation energy for $\text{PbBi}_6\text{As}_2\text{O}_{15}$ at different atmospheres	4.46

4.14	First 30 lines of the indexed X-ray diffraction pattern for orthorhombic $\text{SrBi}_6\text{V}_2\text{O}_{15}$ with $a = 23.9122(4) \text{ \AA}$, $b = 17.1561(3) \text{ \AA}$, $c = 11.1001(2) \text{ \AA}$ and $\alpha = \beta = \gamma = 90^\circ$, $V = 4553.733(237) \text{ \AA}^3$	4.56
4.15	Synthesis temperatures of x in $\text{Pb}_{1-x}\text{Sr}_x\text{Bi}_6\text{As}_2\text{O}_{15}$	4.60
4.16	Melting points of x in $\text{Pb}_{1-x}\text{Sr}_x\text{Bi}_6\text{V}_2\text{O}_{15}$	4.63
4.17	Atomic % of the elements determined from ICP-AES analysis of selected samples in $\text{Pb}_{1-x}\text{Sr}_x\text{Bi}_6\text{V}_2\text{O}_{15}$ solid solutions	4.64
4.18	Grain size of $\text{Pb}_{1-x}\text{Sr}_x\text{Bi}_6\text{V}_2\text{O}_{15}$	4.67
4.19	Grain size of $\text{Pb}_{1-x}\text{Sr}_x\text{Bi}_6\text{As}_2\text{O}_{15}$	4.69
4.20	Melting points of x in $\text{NaBi}_{13}\text{V}_{4-x}\text{As}_x\text{O}_{30}$	4.92
4.21	Melting points of x in $\text{NaBi}_{13}\text{As}_{4-x}\text{P}_x\text{O}_{30}$	4.92
4.22	Melting points of x in $\text{NaBi}_{13}\text{V}_{4-x}\text{P}_x\text{O}_{30}$	4.93
4.23	Atomic % of the elements determined from ICP-AES analysis of selected samples in $\text{NaBi}_{13}\text{V}_{4-x}\text{As}_x\text{O}_{30}$ solid solutions	4.93
4.24	Grain size of $\text{NaBi}_{13}\text{V}_4\text{O}_{30}$ and $\text{NaBi}_{13}\text{As}_4\text{O}_{30}$	4.98
4.25	Grain size of x in $\text{NaBi}_{13}\text{V}_{4-x}\text{As}_x\text{O}_{30}$	4.98
4.26	Grain size of x in $\text{NaBi}_{13}\text{V}_{4-x}\text{P}_x\text{O}_{30}$	4.98
4.27	Melting points of x in $\text{PbBiV}_{2-x}\text{As}_x\text{O}_5$	4.123
4.28	Atomic % of the elements determined from ICP-AES analysis of $\text{PbBi}(\text{V}/\text{As})\text{O}_5$	4.126
4.29	Crystallographic data of different phases of Pb_2BiVO_6 (Mizrahi et al., 1995)	4.142
4.30	Melting points of $\text{Pb}_2\text{BiP}_{1-x}\text{V}_x\text{O}_6$ solid solutions	4.155
4.31	Melting points of $\text{Pb}_2\text{BiP}_{1-x}\text{As}_x\text{O}_6$ solid solutions	4.155
4.32	Melting points of $\text{Pb}_2\text{BiV}_{1-x}\text{As}_x\text{O}_6$ solid solutions	4.156
4.33	Atomic % of the elements determined from ICP-AES analysis of $\text{Pb}_2\text{Bi}(\text{V}/\text{P}/\text{As})\text{O}_6$	4.157

4.34	DTA transitions of $\text{Pb}_2\text{BiP}_{1-x}\text{V}_x\text{O}_6$, $\text{Pb}_2\text{BiV}_{1-x}\text{As}_x\text{O}_6$ and $\text{Pb}_2\text{BiP}_{1-x}\text{As}_x\text{O}_6$ solid solutions	4.163
4.35	Grain size of x in $\text{Pb}_2\text{BiP}_{1-x}\text{V}_x\text{O}_6$	4.167
4.36	Grain size of x in $\text{Pb}_2\text{BiV}_{1-x}\text{As}_x\text{O}_6$	4.167
4.37	Grain size of x in $\text{Pb}_2\text{BiP}_{1-x}\text{As}_x\text{O}_6$	4.168
4.38	Cell parameters of Pb_4BiVO_8 , Pb_4BiPO_8 and $\text{Pb}_4\text{BiAsO}_8$ and reported values	4.188
4.39	Melting points of $\text{Pb}_4\text{BiP}_{1-x}\text{V}_x\text{O}_8$, $\text{Pb}_4\text{BiV}_{1-x}\text{As}_x\text{O}_8$ and $\text{Pb}_4\text{BiP}_{1-x}\text{As}_x\text{O}_8$ solid solutions	4.198
4.40	Atomic % of the elements determined from ICP-AES analysis of $\text{Pb}_4\text{Bi(V/P/As)O}_8$	4.199

CHAPTER 1

INTRODUCTION

1.1 Ionic Conductivity and Solid Electrolytes

Electrical conduction in solid materials usually occurs by the long range diffusion of either electrons or ions. This has therefore created many different characteristics of electrical conductivity, such as metallic conductivity, superconductivity, semiconductivity and ionic conductivity.

Ionic conductivity occurs in materials known variously as solid electrolytes, superionic conductors or fast ion conductors. Many of the crystalline materials such as NaCl or MgO, have low ionic conductivities because the atoms or ions can only vibrate at their atomic positions. However, solid electrolytes are an exception. Solid electrolytes usually have freely moving cations (e.g. H^+ , Na^+ , Li^+ , Ag^+) or anions (e.g. O^{2-} , F^-) that move throughout the crystalline structure.

Figure 1.1 shows the different types of electrical conductivities and examples of the different materials. Solid electrolytes have conductivities that fall between that of the semiconductor and aqueous electrolyte.

Solid electrolytes are, therefore, intermediate between normal crystalline solids with regular three dimensional structures as well as immobile atoms or ions and liquid electrolytes, which do not have regular structures but mobile ions. This characteristic is supported by data on the relative entropies of polymorphic transitions and melting.

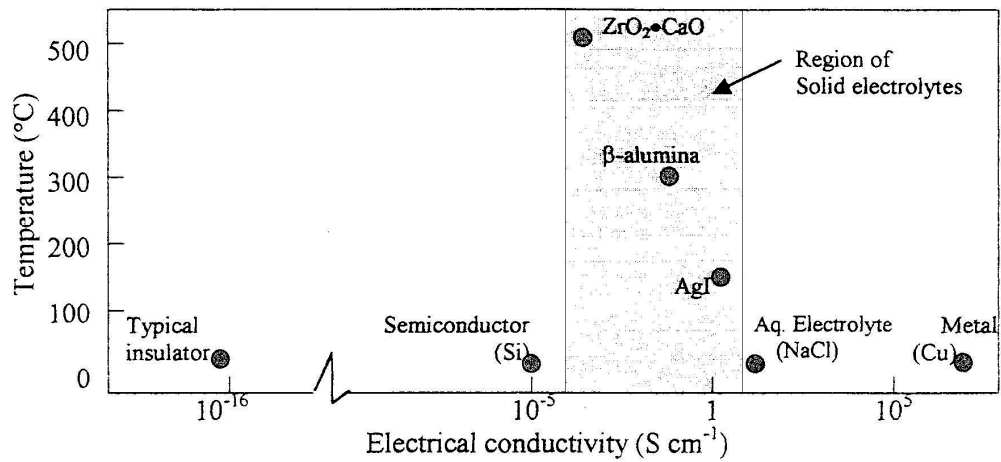


Figure 1.1: Electrical conductivities of selected common substances and representative solid electrolytes (Greenblatt, 1994)

Solid electrolytes are often stable only at high temperatures. At low temperatures, they may undergo a phase transition to give a polymorph with a low ionic conductivity and a more usual type of crystalline structure (Figure 1.2). Besides, solid electrolytes may also form as a consequence of a gradual increase in defect concentration with increasing temperature.

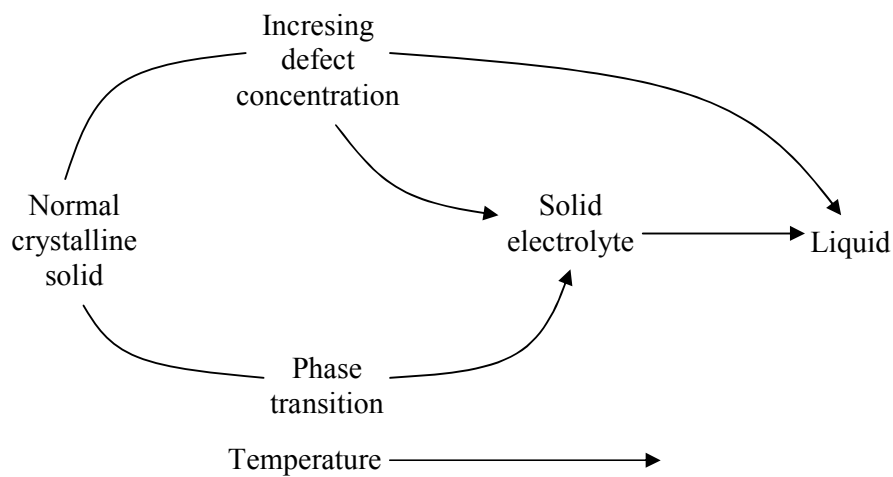


Figure 1.2: Solid electrolytes as intermediate between normal crystalline solids and liquids (West, 1999)

Intensive research has been carried out on solid electrolytes in recent years as these materials offer a wide range of potential technological applications, such as high-energy-density batteries, fuel cells, sensors, electrochromic materials for both optical display and ‘smart window’ devices, low-cost electrolysis of water and selective atomic filter. Some of these devices are available commercially. For example, oxygen detectors for automotive pollution-control systems employ solid O^{2-} conductors and Li^+ batteries for electronic equipment.

1.1.1 Ionic Conduction

The electrical conductivity is defined as the constant of proportionality between the flux j of charge and the electric field, E

$$j = \sigma E \quad (1.1)$$

If

$$j = e_i J \quad (1.2)$$

with e_i = charge of the conducting species, i

J = density of the current

and

$$\mu_i = \frac{J}{n_i E} \quad (1.3)$$

where μ_i = mobility of the species

n_i = number of charge carrier

therefore, for any material and charge carrier, the specific conductivity is given by

$$\sigma = \sum_i n_i e_i \mu_i \quad (1.4)$$

For ionic conductivity,

$$\sigma = N_{\text{ion}} e \mu_{\text{ion}} \quad (1.5)$$

where N_{ion} = number of ions which can change their position under the influence of an electric field

μ_{ion} = the mobility of these ions

(Elliott, 1998; West, 1999)

In order for the ions to move through a crystalline solid, they must have sufficient energy to pass over an energy barrier and there must be empty lattice sites for the ions to jump into. Thus, for an intrinsic conduction, N_{ion} depends on the vacancy concentration caused by Schottky or Frenkel defects.

Transference number, t_i is defined as the ratio of the partial current generated by migration of species i to the total current generated by all conductive species.

Therefore,

$$t_i = \frac{\sigma_i}{\sum_i \sigma_i} \quad (1.6)$$

For an ideal ionic conductor, transference number $t_i = 1$ (Kudo and Fueki, 1989).

Conductivities are usually temperature dependent, and for all materials, except metals, the conductivity increases with increasing temperature.

The temperature dependence of ionic conductivity is usually given by the Arrhenius equation, where graphs of $\log_e \sigma$ against T^{-1} should give straight lines of slope $-\frac{E_a}{R}$.

$$\sigma = A \exp\left(\frac{-E_a}{RT}\right) \quad (1.7)$$

where E_a = activation energy

R = universal gas constant

T = absolute temperature, K

A = pre-exponential factor, which depends on the vibrational frequency of the potentially mobile ions and some structural parameters

(West, 1999)

For an ionic conduction to take place, there are certain conditions that must be satisfied:

1. A large number of the ions of one species should be mobile (i.e. a large value of n in the equation $\sigma = ne\mu$).
2. There should be a large number of empty sites available for the mobile ions to jump into.
3. The empty and occupied sites should have similar potential energy with a low activation barrier for jumping between neighbouring sites.
4. The structure should have a framework, preferably 3D, permeated by open channels through which mobile ions may migrate.
5. The anion framework should be highly polarisable.

Even when all these conditions are met, the ionic conduction may still be affected by microstructural factors such as grain boundaries, grain size, pores size and between grain-grain contact. However, these effects have not been studied experimentally in great detail.

1.2 Solid Solutions

A solid solution is basically a crystalline phase that can have variable composition. As with doped crystals, simple solid solutions are divided into two types: substitutional solid solutions in which the atom or ion that is being introduced directly replaces an atom or ion in the parent structure and interstitial solid solutions in which the introduced species occupies a site that is normally empty and no ions or atoms are left out.

Doping is an important mechanism in preparing solid solutions. Usually, doping with aliovalent cations (the substituted ions are ions of different charge) will result in creation of vacancies or interstitials (ionic compensation) or electrons or holes (electronic compensation). Therefore, substituting a cation of lower valence may result in creating anion vacancies, thus, increasing the oxygen vacancies in the oxide ion conductor and consequently increasing the conductivity.

In solid solution formation, ions of similar size may substitute for each other easily and extensive solid solutions could form which are stable at all temperatures; the enthalpy of mixing of such similar-sized ions is likely to be small and the driving force for solid solution formation is the increased entropy. Solid solutions may form

at high temperatures if substituting ions differ in size by 15 to 20%, where the entropy term is able to offset the positive enthalpy term. With ions that differ in size by more than $\sim 30\%$, however, solid solutions are normally not expected to form.

Solid solution formation is very temperature dependent. Thus, extensive solid solutions often form at high temperatures whereas at lower temperatures, these may be more restricted or practically non-existent.

In order to form a complete solid solution, it is essential that the end members are isostructural; however, the reverse is not necessarily true.

1.3 Oxide Ion Conductors and Their Applications

A very interesting subgroup of solid electrolytes is the materials that display oxygen ion conductivity, known as oxide ion conductors, where the oxide ions are the charge carriers.

Oxide ion conductors have been with us for over a century. The first application was by Nerst in around 1900, who used stabilised zirconia as filaments in his revolutionary 'glower' electric lights, driven by the need to replace dirty and dangerous candles and gas lamps. Remarkably, the same basic material, now known as yttria-stabilised zirconia, is the key solid electrolyte component currently in various solid oxide fuel cell and sensor applications.